Synergistic Highly Potent Targeted Drug Combinations in different Pheochromocytoma Models including Human Tumor Cultures

Fankhauser, Maria ; Bechmann, Nicole ; Lauseker, Michael ; Goncalves, Judith ; Favier, Judith ; Klink, Barbara ; William, Doreen ; Gieldon, Laura ; Maurer, Julian ; Spöttl, Gerald ; Rank, Petra ; Knösel, Thomas ; Orth, Michael ; Ziegler, Christian G ; Aristizabal Prada, Elke Tatjana ; Rubinstein, German ; Fassnacht, Martin ; Spitzweg, Christine ; Grossman, Ashley B ; Pacak, Karel ; Beuschlein, Felix ; Bornstein, Stefan R ; Eisenhofer, Graeme ; Auernhammer, Christoph J ; Reincke, Martin ; Nölting, Svenja

Abstract: There are no officially approved therapies for metastatic pheochromocytomas apart from ultratrace 131I-MIBG therapy approved only in the United States. We have, therefore, investigated the anti-tumor potential of novel molecular-targeted approaches in murine pheochromocytoma cell lines (MPC/MTT), immortalized mouse chromaffin Sdhb-/- cells, 3D-pheochromocytoma tumor models (MPC/MTT spheroids) and human pheochromocytoma primary cultures. We identified the specific PI3K inhibitor BYL719 and the mTORC1 inhibitor everolimus as the most effective combination in all models. Single treatment with clinically relevant doses of BYL719 and everolimus significantly decreased MPC/MTT and Sdhb-/- cell viability. A targeted combination of both inhibitors synergistically reduced MPC and Sdhb-/- cell viability and showed an additive effect on MTT cells. In MPC/MTT spheroids, treatment with clinically relevant doses of BYL719 alone or in combination with everolimus was highly effective, leading to a significant shrinkage or even a complete collapse of the spheroids. We confirmed the synergism of clinically relevant doses of BYL719 plus everolimus in human pheochromocytoma primary cultures of individual patient tumors with BYL719 attenuating everolimus-induced AKT activation. We have thus established a method to assess molecular-targeted therapies in human pheochromocytoma cultures and identified a highly effective combination therapy. Our data pave the way to customized combination therapy to target individual patient tumors.

DOI: https://doi.org/10.1210/en.2019-00410

Highly Potent Targeted Drug Combinations in different Pheochromocytoma Models including Human Tumor Cultures. Endocrinology, 160(11):2600-2617.
DOI: https://doi.org/10.1210/en.2019-00410

Synergistic Highly Potent Targeted Drug Combinations in Different Pheochromocytoma Models including Human Tumor Cultures

Maria Fankhauser, Nicole Bechmann, Michael Lauseker, Judith Goncalves, Judith Favier, Barbara Klink, Doreen William, Laura Gieldon, Julian Maurer, Gerald Spöttl, Petra Rank, Thomas Knösel, Michael Orth, Christian G. Ziegler, Elke Tatjana Aristizabal Prada, German Rubinstein, Martin Fassnacht, Christine Spitzweg, Ashley B. Grossman, Karel Pacak, Felix Beuschlein, Stefan R. Bornstein, Graeme Eisenhofer, Christoph J. Auernhammer, Martin Reincke and Svenja Nölting

Endocrinology
Endocrine Society

Submitted: May 30, 2019
Accepted: July 14, 2019
First Online: July 19, 2019

 DOI: 10.1210/js.2019-00178

SYNERGISTIC HIGHLY POTENT TARGETED DRUG COMBINATIONS IN DIFFERENT PHEOCHROMOCYTOMA MODELS INCLUDING HUMAN TUMOR CULTURES

Maria Fankhauser[1*], Nicole Bechmann[2*], Michael Lauseker[3], Judith Goncalves[4,5,6], Judith Favier[4,5], Barbara Klink[7,8,9], Doreen William[9], Laura Gieldon[7,9], Julian Maurer[1], Gerald Spöttl[1], Petra Rank[1], Thomas Knösel[10], Michael Orth[11], Christian G. Ziegler[12], Elke Tatjana Aristizabal Prada[1], German Rubinstein[1], Martin Fassnacht[13], Christine Spitzweg[1], Ashley B. Grossman[14,15], Karel Pacak[16], Felix Beuschlein[1,17], Stefan R. Bornstein[12], Graeme Eisenhofer[2,12], Christoph J. Auernhammer[1], Martin Reincke[1] and Svenja Nölting[1]

[1]*Medizinische Klinik und Poliklinik IV, Klinikum der Universität, LMU München, Munich, Germany*

[2]*Institute for Clinical Chemistry and Laboratory Medicine, University Hospital Carl Gustav Carus at Technische Universität Dresden, Dresden, Germany,*

[3]*Institute for Medical Information Sciences, Biometry, and Epidemiology, Campus Grosshadern, Ludwig-Maximilians-University of Munich, Munich, Germany*

[4]*INSERM, UMR970, Paris-Cardiovascular Research Center, Equipe Labellisée par la Ligue contre le Cancer, F-75015, Paris, France.*

[5]*Université Paris Descartes, Sorbonne Paris Cité, Faculté de Médecine, F-75006 Paris, France*

[6]*Université Paris Diderot, Sorbonne Paris Cité, F-75013 Paris, France*

[7]*Institute for Clinical Genetics, Faculty of Medicine Carl Gustav Carus, TU Dresden, Fetscherstrasse 74, D-01307 Dresden, Germany*

[8]*National Center of Genetics (NCG), Laboratoire national de santé (LNS), 1, rue Louis Rech, L-3555 Dudelange, Luxembourg*

[9]*German Cancer Consortium (DKTK), Dresden, Germany; German Cancer Research Center (DKFZ), Heidelberg, Germany; Core Unit for Molecular Tumor Diagnostics (CMTD), National Center for Tumor Diseases (NCT), Germany*

[10]*Institute of Pathology, Ludwig-Maximilians-University, Munich, Germany*

[11]*Department of Radiation Oncology, University Hospital, LMU Munich, Munich, Germany*

[12]*Department of Medicine III, University Hospital Carl Gustav Carus Dresden, Germany*

[13]*Department of Medicine I, Division of Endocrinology and Diabetology, University Hospital, University of Würzburg, Würzburg, Germany*

[14]*Oxford Centre for Diabetes, Endocrinology and Metabolism, University of Oxford, Oxford, UK*

[15]*Royal Free Hospital ENETS Centre of Excellence, London, UK*

[16]*Eunice Kennedy Shriver National Institute of Child Health and Human Development, National Institutes of Health, Bethesda, Maryland, USA*

[17]*Klinik für Endokrinologie, Diabetologie und Klinische Ernährung, Universitätsspital Zürich, Zurich, Switzerland*

ORCiD numbers:

0000-0002-7064-590X

Nölting

Svenja

Received 30 May 2019. Accepted 14 July 2019.
*These authors contributed equally to this work

There are no officially approved therapies for metastatic pheochromocytomas apart from ultratrace ^{131}I-MIBG therapy approved only in the United States. We have, therefore, investigated the anti-tumor potential of novel molecular-targeted approaches in murine pheochromocytoma cell lines (MPC/MTT), immortalized mouse chromaffin *Sdhb-/-* cells, 3D-pheochromocytoma tumor models (MPC/MTT spheroids) and human pheochromocytoma primary cultures. We identified the specific PI3Kα inhibitor BYL719 and the mTORC1 inhibitor everolimus as the most effective combination in all models. Single treatment with clinically relevant doses of BYL719 and everolimus significantly decreased MPC/MTT and *Sdhb-/-* cell viability. A targeted combination of both inhibitors synergistically reduced MPC and *Sdhb-/-* cell viability and showed an additive effect on MTT cells. In MPC/MTT spheroids, treatment with clinically relevant doses of BYL719 alone or in combination with everolimus was highly effective, leading to a significant shrinkage or even a complete collapse of the spheroids. We confirmed the synergism of clinically relevant doses of BYL719 plus everolimus in human pheochromocytoma primary cultures of individual patient tumors with BYL719 attenuating everolimus-induced AKT activation. We have thus established a method to assess molecular-targeted therapies in human pheochromocytoma cultures and identified a highly effective combination therapy. Our data pave the way to customized combination therapy to target individual patient tumors.

1. Introduction

Pheochromocytomas and paragangliomas (PCCs/PGLs) are rare neuroendocrine, catecholamine-producing tumors that originate from the adrenal medulla or extra-adrenal paraganglia. About 10% of PCCs and 35-40% of PGLs are metastatic (1-9). The prognosis of patients with metastatic PCC/PGL is poor, with a 5-year survival rate of 63% (10). Current therapeutic approaches for metastatic PCC/PGL, such as radionuclide therapy with ^{131}I-metaiodbenzylguanidine **(**MIBG), peptide receptor radionuclide therapy (PRRT) (11), or chemotherapy, are - apart from ultratrace ^{131}I-MIBG approved only in the United States - not officially approved and are limited in their effectiveness, as recently reviewed (12). Therefore, novel therapeutic strategies are urgently needed.

The standard chemotherapy regime for PCC/PGLs is CVD (cyclophosphamide, vincristine, dacarbazine). Inhibitors of the DNA repair enzyme poly(ADP-ribose) polymerase (PARP) have been demonstrated to potentiate DNA damaging effects of alkylating chemotherapeutic agents such as dacarbazine or temozolomide (13-15), both being metabolized to the same active metabolite (16). Therefore, combining standard chemotherapy with a PARP inhibitor might be a promising novel therapeutic approach.

Another therapeutic approach is to define the aberrant molecular pathways in such tumors which can then be targeted by specific therapy. In around 30-40% of PCC/PGL patients germline mutations can be identified, with an equal number showing somatic mutations in more than 20 well-characterized susceptibility genes (17,18). These different mutations can be separated into three main molecular clusters (summarized in Fig. 1 and recently reviewed (19)):

i) The pseudohypoxic signaling cluster (cluster-1)supple is related to mutations of genes encoding for proteins that are associated with significant regulation of the hypoxia signaling pathway; these include mutations in genes encoding for hypoxia-inducible factor-2α (*HIF2A*), Krebs cycle enzymes such as succinate dehydrogenase subunits (*SDHx* [*SDHA, SDHB, SDHC, SDHD*]), succinate dehydrogenase complex assembly factor-2 (*SDHAF2*), fumarate hydratase (*FH*), malate dehydrogenase 2 (*MDH2*), and isocitrate dehydrogenase 1 (*IDH1*). This pathway also includes mutations in von Hippel–Lindau tumor suppressor (*VHL*) and egl-9 prolyl hydroxylase-1 and -2 (*EGLN1/2*) genes. Such mutations promote HIF-α stabilization and accumulation resulting, amongst other effects, in increased angiogenesis via changes in vascular endothelial growth factor-1 and -2 receptors (VEGFR1/2) and platelet-derived growth factor-β receptor (PDGFR) transcription.

ii) The kinase signaling cluster (cluster-2) is related to mutations of genes encoding for proteins that belong to the phosphatidylinositol-3-kinase/mammalian target of rapamycin (PI3K/mTORC1) pathway/receptor kinase signaling, and comprises mutations in the rearranged-during-transfection (*RET)* proto-oncogene, neurofibromin 1 (*NF1*) tumor suppressor, *H-RAS* and *K-RAS* proto-oncogenes, transmembrane protein 127 (*TMEM127*) and Myc-associated factor X (*MAX*).

iii) Most recently, the Wnt signaling cluster (cluster-3) has been described as being of pathological significance.

The multi-targeted receptor tyrosine kinase inhibitor (TKI) sunitinib has anti-angiogenic and anti-proliferative potential due to inhibition of VEGFR1/2, PDGFR, and RET, and has been approved for the treatment of renal cell carcinomas, pancreatic neuroendocrine tumors (NETs) and gastrointestinal stromal tumors. Sunitinib is currently being investigated in the first randomized placebo-controlled phase II clinical trial in PCC/PGL patients, in which recruitment has been completed (FIRST-MAPPP, NCT01371202).

The mTORC1 inhibitor everolimus, currently used in the treatment of breast cancer, renal cell carcinoma and NETs, showed poor efficacy when used alone in PCC/PGLs (20). However, one *SDHB*-mutated patient who was treated with the combination of low doses of the mTORC1 inhibitor rapamycin and the TKI sunitinib showed maintained long-term disease control (21).

In an *in vivo* breast cancer mouse model, the mTORC1 inhibitor everolimus has shown synergistic effects together with the PI3Kα inhibitor BYL719 (alpelisib) and overcame BYL719 resistance (22). The clinical phase III approval study SOLAR-1 investigating BYL719 in breast cancer patients has reached its final endpoints (23). Moreover, BYL719 overcame everolimus resistance in a stably everolimus-resistant pancreatic NET cell line model (24). Therefore, combining different targeted drugs may strongly enhance their therapeutic potential and prevent the development of resistance.

Based on these data, we have investigated the anti-tumor potential of a variety of both targeted and chemotherapeutic agents and their combinations, and their impact on cellular signaling pathways, in well-validated murine PCC cell line models and a murine *Sdhb* knock-out (*Sdhb-/-*) cell line (the best available cell line models for highly aggressive *SDHB*-mutated paragangliomas), 3D murine PCC spheroids and human PCC primary cultures, in order to identify novel therapeutic options.

2. Materials and methods

2.1 Cell lines

Murine MPC (MPC 4/30/PRR) (25) and MTT (26) cell lines were cultured, as described previously (27) in DMEM/F12 (1:1) (Life Technologies, Karlsruhe, Germany), supplemented with 10% FBS (Biochrom, Berlin, Germany), 1% penicillin/streptomycin (Life Technologies) and 0.4% amphotericin B (Biochrom, Berlin, Germany) at 5% CO_2 and 37°C. Cells were counted by an automated cell counter (Countess, Invitrogen, Germany). MPC/MTT cells were confirmed for species identity by cytochrome C oxidase I DNA barcoding, and for strain identity by comparing short tandem repeats (STRs) from these cell lines with STRs of identity-confirmed counterparts, as described previously (28). These analyses were performed by the DSMZ (Braunschweig, Germany).

Immortalized mouse chromaffin cells both wild-type (WT) and *Sdhb-/-* (29) were cultured in DMEM Glutamax (Dulbecco Modified Eagle Medium, Gibco) with 10% FBS (Fetal bovine serum, Gibco) and 1% antibiotics (penicillin/streptomycin, Gibco) at 37°C in 5% CO_2.

2.2 Inhibitors

Everolimus, BYL719, sunitinib, temozolomide, niraparib (PARP inhibitor), cabozantinib (a TKI inhibiting c-met/VEGFR2/c-KIT/FLT3/RET/TIE2) and entinostat (a histone deacetylase (HDAC) 1/3 inhibitor) were purchased from Selleckchem (Munich, Germany). All drugs

were dissolved in DMSO (Sigma, D8418) and diluted in 0.2% bovine serum albumin (BSA)/PBS. DMSO was used as the vehicle (DMSO control) equal to the highest dose of each single experiment, and had no effect on cell viability up to concentrations of 0.2% (1:500) DMSO.

2.3 Dose finding: Clinically relevant doses

Treatment doses of 10-25nM everolimus were chosen since the plasma levels in patients on daily therapy with 10mg everolimus range between approximately 8nM (c_{min} after 2 weeks of daily exposure to 10mg everolimus) and 59nM (c_{2h} after 12 weeks of daily exposure to 10mg everolimus) (30).

Concentrations of 2.5µM-10µM BYL719 utilized in our experiments are also clinically relevant: in patients with advanced solid malignancies, median BYL719 plasma concentrations between 2µM and 11µM were found 2-8h post dose with one-month daily oral standard therapy with 300-450mg BYL719 (31).

We used 0.5-2µM sunitinb in MPC/MTT cells and in human PCC cultures. Administration of 50mg sunitinib per day leads to plasma concentrations of 0.1–0.2µM (32). Thus, we only used a slightly higher dose as our starting concentration.

We used 0.5-2µM cabozantinib in MPC/MTT cells and 1-10µM cabozantinib in human PCC cultures. Administration of 20-60mg of cabozantinib per day leads to plasma concentrations of 0.7-2.2µM (33).

2.4 Human PCC primary cultures

This study was approved by ENS@T – the *European Network for the Study of Adrenal Tumors*, and informed consent was obtained from each patient. Primary tumor tissues were isolated from adrenal glands of six different PCC patients, and lymph node/uterus metastases were isolated from one metastatic PGL patient (n=7). Specimens were taken immediately after surgery, and placed into Petri dishes filled with PBS. Tissue was separated into 0.5mm pieces. Diced tissue was resuspended in 10ml collagenase (Biochrom, Berlin, Germany) and incubated at 37°C for 60 min. Subsequently, 2ml pure FCS were added to inactivate the collagenase, and tumor tissue was centrifuged at 1100 rpm for 5 min. Supernatant was removed, and the pellet gently resuspended in erythrocyte lysis buffer. After 7 min. incubation, centrifugation was repeated, supernatant was removed and the pellet was resuspended in DMEM/F12 supplemented with 10% FCS, 1% penicillin/streptomycin and 0.4% amphotericin B. Suspension was filtered through a 70µm sieve, cells were counted and seeded into 96-well or 6-well plates. After 3-5 days of incubation, cells were treated with everolimus, BYL719, sunitinib, temozolomide, niraparib, cabozantinib or entinostat. After 48h or 72h, cell viability was analyzed. To confirm chromaffin cell origin, we used Western blot analysis of synaptophysin after 24h, as described below.

2.5 Cell viability

MPC/MTT cells were seeded into 96-well plates at densities of 2000 cells per well, grown for 24h, and treated with different concentrations of sunitinib, BYL719 and cabozantinib, either alone or in combination with everolimus. Furthermore, cells were treated with niraparib alone or in combination with temozolomide or with entinostat alone. Metabolic activity was assessed by the "Cell Titer Blue®" cell viability assay (#G8081, Promega, Madison, WI, USA) after 48h, 72h and 120h of drug incubation. Cells were incubated for 4h with Cell Titer Blue® solution; fluorescence was measured at 560/590nm using a GLOMAX plate reader (Promega).

2.6 Cell Cycle Analysis

The cell cycle was analyzed (BD Accuri C6 Analysis), as previously described (24). For Flow Cytometric Analysis (FACS) analysis, cells were incubated for 24h with BYL719, everolimus and sunitinib alone or in combination.

2.7 Apoptosis

Apoptosis was measured after 24h treatment with BYL719, everolimus and sunitinib, alone or in combination, using the Apo-One homogeneous caspase3/7-Assay kit (#G7790, Promega), as previously described (24).

2.8 Cytotoxicity by crystal violet assay (CVA)

2.5×10^3 cells/well were seeded into 48-well plates and treated for 72h (everolimus, BYL719, combination or vehicle). Crystal violet assay was then performed as previously described (34). Values were standardized to the vehicle absorbance at 24h and expressed as cell viability. Cell viability curves were established. Experiments were performed three times, in duplicates.

2.9 Spheroid cultivation and treatment

Generation and cultivation of MPC/MTT cell spheroids was conducted, as described previously (35,36). Four days after spheroid generation, spheroids were treated with sunitinib or BYL719 alone or in combination with everolimus. Afterwards, spheroid growth was monitored for 14 days (single treatment). During cultivation, medium was replaced every three to four days. Furthermore, a fractionated treatment regime was utilized by additional treatment of the spheroids on days 7, 11, and 14.

2.10 Protein Extraction and Western Blot Analysis

Cells were seeded into 10-cm plates and grown for 24h in complete medium before incubated with sunitinib and BYL719, either alone or in combination with everolimus, for 24h or 48h. Duplicate wells were used for each concentration of drug. Western blotting was conducted as described previously (37),using the following primary and secondary antibodies and their dilutions: pAktT (Ser473) (dilution: 1:20000) (RRID:AB_2315049) (38), AKT (dilution: 1:5000) (RRID:AB_329827) (39), p4EBP1 (Ser65) (dilution: 1:2000) (RRID: AB_330947) (40), 4EBP1 (dilution: 1:1000) (RRID:AB_2097841) (41), p53 (dilution: 1:1000) (RRID: AB_10695803) (42), cyclin D1 (dilution: 1:1000) (RRID:AB_2259616) (43), cyclin D3 (dilution: 1:2000) (RRID:AB_2070801) (44), pp70S6K (Thr389) (dilution: 1:1000) (RRID:AB_330944) (45), p70S6K (dilution: 1:5000) (RRID:AB_390722) (46), pS6 (Ser240/244) (dilution: 1:200000) (RRID:AB_10694233) (47), S6 (dilution: 1:20000) (RRID:AB_331355) (48), pGSK3α/β (Ser21/9) (dilution: 1:5000) (RRID: AB_329830) (49), GSK3α/β (dilution: 1:1000) (RRID:AB_10547140) (50), CDK1/cdc2 (POH1) (dilution: 1:1000) (RRID:AB_2074795) (51), Chk1 (2G1D5) (dilution: 1:000) (RRID:AB_2080320) (52) (Cell Signaling, Danvers, MA, USA), IRS-1 (dilution: 1:5000) (RRID:AB_2536328) (53), pIRS-1 (Ser312) (dilution: 1:5000) (RRID:AB_2533767) (54) (Invitrogen, Carlsbad, USA), actin (dilution: 1:10000) (RRID:AB_476744) (55) (Sigma-Aldrich, St. Louis, USA), and synaptophysin clone SY38 (dilution: 1:1000) (RRID:AB_95187) (56) (Merck-Millipore, Darmstadt, Germany). Western blot quantification was performed and a representative blot of three independent experiments is shown.

2.11 Multi-gene panel next generation sequencing (NGS)

Testing for disease-causing variants in PCC/PGL associated genes was performed by targeted next-generation sequencing (NGS), as described previously (57) using a custom designed multi-gene panel based on the TruSeq® Nano DNA Library Prep Kit (Illumina, San Diego, CA, USA).

The panel comprises 84 genes including more than 20 genes associated with PCC/PGL (supplementary Table 1 (58)), and was shown to be suitable for analysis of blood and formalin fixed paraffin embedded (FFPE) or fresh frozen tumor tissue. DNA was isolated from formalin-fixed paraffin-embedded tumor tissue samples. Library preparation was done according to the manufacturer`s instructions and 150 nt paired-end sequencing was carried out with a minimum median coverage of 1000-fold on a *NextSeq500* sequencer (Illumina).

Data analysis was performed using the Biomedical Genomics Workbench 5.0 (Qiagen), as described previously (59). Settings for variant calling in tumor tissue were adapted using a low frequency variant detection algorithm with a required minimum frequency of 5%, three reads supporting the variant and a required minimum coverage of ten reads.

2.12 Statistical Analysis

Results are displayed as mean ± standard deviation of the mean (SD) of at least three independent experiments. Each cell viability experiment consisted of at least six samples per concentration and incubation time. Cell viability in the MCP/MTT experiments was modeled via a linear mixed model with random effects for trial and fixed effects for substances and their interactions. For the human primary cultures we used a linear mixed model for the natural logarithm of the viability. *Synergism* was assessed, as described previously (60), and was confirmed when both single effects were significant, the interaction effect was significant, and all regression coefficients were negative. When both single effects were significant and the interaction effect was not significant, it was defined as an *additive* effect.

For spheroid data, diameter of the spheroids was modeled via a quasi-Poisson mixed model with random effects for trial and spheroid. Temporal correlation was modeled via a continuous AR(1)-correlation structure. Besides the main effects, the model included a quadratic term for the day since starting and interactions between time and substances. All significance tests were performed within the respective model.

Calculations were performed using R 3.5.1 (R Foundation for Statistical Computing, Vienna, Austria). Significance was assessed at $p<0.05$. Due to the exploratory character of this work, we did not adjust any p-values for multiple testing.

3. Results

3.1 MPC/MTT cells

3.1.1 Cell viability after different drug treatments

Treatment (120h) with clinically relevant doses of BYL719 (2.5µM/5µM) and everolimus (10nM), respectively, significantly diminished MPC/MTT cell viability compared to the control (Fig. 2); combination treatment with 5µM BYL719 and 10nM everolimus synergistically reduced MPC and additively MTT reduced cell viability (Fig. 2).

Treatment with sunitinib (1µM/2µM) and everolimus (10nM), respectively, significantly reduced MPC/MTT cell viability compared to the control (Fig. 3). Combination treatment synergistically reduced MPC (1µM/2µM sunitinib plus 10nM everolimus) and MTT (2µM sunitinib plus 10nM everolimus) cell viability (Fig. 3).

Cabozantinib (1µM/2µM) significantly reduced MPC/MTT cell viability (supplementary Fig. S1 (58)), but was not synergistic with everolimus (data not shown).

Niraparib (0.5µM/1µM) and temozolomide (100µM/250µM) singly significantly reduced MPC/MTT cell viability compared to the control (Fig. 4). Combination of 0.5-1µM niraparib plus 100µM temozolomide, or 0.5µM niraparib plus 250µM temozolomide, synergistically diminished MTT, but not MPC, cell viability (Fig. 4).

For all the following experiments in MPC/MTT cells and spheroids, we only investigated the most promising combinations (BYL719/everolimus and sunitinib/everolimus).

3.1.2 Cell cycle and Apoptosis

BYL719 (5µM), everolimus (10nM) and sunitinib (1µM/2µM) significantly increased the G1 cell cycle phase in MPC cells, compared to the control (Fig. 5). In MTT cells everolimus (10nM) and sunitinib (1µM/2µM) significantly increased the G1 cell cycle phase. In both cell lines BYL719/everolimus or sunitinib/everolimus combination treatments further enhanced G1-phase cell cycle arrest, compared to single treatments (Fig. 5). Supplementary Fig. S2 (58) shows the sub-G1-phase.

Apoptosis was investigated by caspase assay. In both cell lines significant apoptosis induction was observed after BYL719 treatment alone (2.5µM/5µM), after BYL719/everolimus combination treatment and – to a lesser extent – after the sunitinib/everolimus combination treatment (Figure 6).

3.1.3 Western blot analysis

Western blot results of MPC/MTT cells are shown in Figure 7. Western blot quantification is shown in supplementary Figure S3 (58). Everolimus is known to inhibit mTORC1/p70S6K and thereby activate AKT. Indeed, everolimus and each combination treatment inhibited p70S6K and S6 in MPC/MTT cells; 4EBP1, another mTORC1 effector, was inhibited by everolimus, BYL719 and each combination treatment. PI3K/AKT_{S473} was activated in response to everolimus, inhibited by BYL719, and unaffected by sunitinib. The BYL719/everolimus combination attenuated everolimus-induced PI3K/AKT_{S473} activation to the level of the untreated control. The sunitinib/everolimus combination did not effectively attenuate everolimus-induced PI3K/AKT_{S473} activation. Although most of the effects were seen at the highest doses tested, it is important to mention that these are still low clinically relevant doses (clinically relevant doses of BYL719 are 2-11µM and of everolimus 8-59nM).

PI3K/AKT phosphorylates and thereby inhibits GSK3 (61). Persistent activation of PI3K leads to feed-back down-regulation of IRS-1, which may in turn lead to GSK3 dis-inhibition/activation (62). GSK3α/β phosphorylation and thereby inhibition led to a significant decrease in NET cell viability (63). In this study BYL719 and everolimus alone led to GSK3 inhibition in MPC/MTT cells, while combination treatment even more strongly inhibited GSK3. The sunitinib/everolimus combination also led to GSK3 inhibition, compared to the control and single treatment in MTT cells, but inhibited GSK3β to a lesser extent than the BYL719/everolimus combination. BYL719 alone, everolimus alone and BYL719/everolimus combination treatment promoted IRS-1 up-regulation in MPC/MTT cells as a potential mechanism of GSK3 inhibition.

Consistent with induction of G1 cell cycle arrest, Cyclin D1 and D3 decreased after BYL719/everolimus and sunitinib/everolimus combination treatments in MPC/MTT cells.

3.2 *Sdhb-/-* immortalized mouse chromaffin cells (imCC)

PCC/PGL patients carrying mutations in *SDHB* often show increased incidence of an early onset, increased metastatic risk, and thus a poor prognosis (64), and effective treatment strategies for these patients are missing. Therefore, we have investigated the impact of BYL719 (2.5µM), and everolimus (10nM) alone or in combination on immortalized mouse chromaffin cells (imCC) with and without expression of *Sdhb*. *Sdhb-/-* imCC carry a true knock-out of the *Sdhb* gene, leading to the absence of SDHB protein and complete inhibition of SDH activity (29). Both everolimus and BYL719 alone significantly reduced *Sdhb-/-* cell viability compared to the vehicle, with a synergistic effect of the combination at 72h (Fig. 8). Moreover, BYL719 treatment alone had a significantly stronger inhibitory effect on *Sdhb-/-* imCC viability compared to WT imCC viability after 48 and 72h treatment, but the combination treatment was no more effective in *Sdhb-/-* than in the WT cells after 72h treatment (Fig. 8).

3.3 MPC/MTT cell spheroids

Tumor cell spheroids are characterized by an oxygen and nutrient gradient and provide an excellent *in vitro* model for drug screening with regard to their anti-tumor activity. Fractionated treatment with clinically relevant doses of BYL719 (5µM) led to a significant shrinkage of MPC/MTT spheroids, compared to the spheroid sizes at the beginning (day 4), and in several cases to complete spheroid collapse (day 16) (Fig. 9, supplementary Fig. S4A/D, S5A/D (58)). Fractionated treatment with clinically relevant doses of everolimus (25nM) significantly inhibited MPC/MTT spheroid growth (Fig. 9, supplementary Fig.

S4A/B/C, S5A/B/C (58)). These effects were enhanced by the BYL719/everolimus combination leading to a significant shrinkage or an early complete collapse of MPC/MTT spheroids in several experiments (day 9 and 14, respectively) (Fig. 9). While the DMSO control had an average diameter of 585±50.2µm (MPC) and 500±166.3µm (MTT) after 18 days, fractionated treatment with 25nM everolimus plus 5µM BYL719 led to a significantly smaller average spheroid diameter of 59.5±68.8µm (MPC) and 62.7±42.3µm (MTT), respectively. Fractionated treatment with sunitinib only slowed spheroid growth down (supplementary Fig. S4B/C, S5B/C (58)). In MPC spheroids, sunitinib enhanced the efficacy of everolimus (supplementary Fig. S4B/C/F/G (58)), but not in MTT spheroids after fractionated treatment (supplementary Fig. S4B/C (58)). Fractionated treatment was more effective than single treatment. No spheroid re-growth was seen after BYL719 single treatment.

3.4 Human primary cultures

3.4.1 Clinical, histological and genetic characteristics (Table 1)

We were able to generate primary cultures from seven different PCC/PGL patients, and confirmed tumor identity by detecting synaptophysin as a well-established PCC/PGL marker [30].

Tumors from patients 1, 2, 4 and 6 showed certain criteria associated with an adverse prognosis including capsule invasion, vascular invasion, a size of >5 cm, or a Ki-67 of 5% (Table 1), although they were not metastatic. Patient 7 had a metastatic PGL.

Targeted NGS (Table 1) showed disease-causing *NF1* mutations in tumors of patients 2 and 3, in line with cluster 2 tumors. These were likely somatic mutations; in neither patient was germline testing available, but neither showed any clinical stigmata of neurofibromatosis. However, to completely exclude the possibility of a hereditary PPGL syndrome, pathogenic variants identified in tumor tissue would need to be analyzed in corresponding blood samples as well.

In tumor tissue from patient 7, we identified a missense variant of unknown significance (VUS) in the *Tet Methylcytosine Dioxygenase (TET1)* gene, a demethylase involved in epigenetic regulation and gene activation. In the tumor tissues from patients 1 and 4, no known disease-causing susceptibility mutation was identified by NGS. NGS was not performed on tumor tissues from patients 5 and 6.

3.4.2 Primary cell culture viability after different drug treatments

We have statistically combined all human tumor cultures in which combination treatments were tested (tumor cultures from six different patients, n=6).

In all combination-treated human primary cultures (n=6), clinically relevant doses of BYL719 (2.5µM/5µM) and everolimus (10nM) significantly reduced viability, and the combination of 5µM BYL719 and 10nM everolimus was highly effective and synergistic ($P<0.05$) (Fig. 10).

Sunitinib (2µM) significantly decreased primary culture viability, but was not synergistic with everolimus (Fig. 10).

We could not test combination treatments in the primary cultures from patient 7 as there was insufficient tissue material. Sunitinib (1-8µM) and clinically relevant doses of BYL719 (2.5-10µM) separately decreased viability of the primary cultures from patient 7 (supplementary Fig. S6 (58)).

Furthermore, we were able to test entinostat (1-10µM), cabozantinib (1-10µM), niraparib (5-10µM) and temozolomide (100-250µM) in primary cultures from five different PCC patients. Entinostat (1-10µM), cabozantinib (1-10µM) and niraparib (5-10µM) significantly decreased primary culture viability, but temozolomide had no effect (Fig. 11).

3.4.3 Western blot analysis

We had sufficient human primary culture material from patients 2, 3 and 5 for performing detailed Western blot analysis of these primary cultures; the results are shown in Fig. 12. Western blot quantification of the treatments performed identically in all three primary cultures (control DMSO, 10nM everolimus, 2µM BYL719, BYL719/everolimus combination) is shown in supplementary Fig. S7 (58). Supplementary Table 2 (58) shows all the values of the Western blot quantification of all primary culture Western blots. The mTORC1 effector proteins p70S6K and S6 were strongly inhibited by everolimus and by each combination treatment at 24h; 4EBP1, another mTORC1 effector protein, was inhibited by everolimus and the BYL719/everolimus combination treatment. AKT_{S473} was activated in response to everolimus, and this activation was attenuated by addition of BYL719 in the primary cultures from patients 3 and 5. In contrast to the mouse cell lines, inhibition of GSK3 by BYL719 or by combination treatments could not be shown, possibly due to a shorter treatment time of 24h. However, after a longer incubation time of 48h, the protein concentration of the primary cultures was too low for Western blot detection. P53 was moderately down-regulated by the everolimus/BYL719 combination. Consistent with a G1-phase cell cycle arrest, combination treatments were associated with down-regulation of the cell cycle promoting markers cyclin D3, CDK1 cdc2 (patient 3) and chk1 (patients 3, 5).

4. Discussion

We have shown that targeted combination treatment with clinically relevant doses of the PI3Kα inhibitor BYL719 and the mTORC1 inhibitor everolimus exhibited strong synergistic anti-tumor potential in PCC cell lines and especially *Sdhb-/-* cells, and in human PCC primary cultures. In MPC/MTT 3D-spheroids, this combination treatment led to dramatic spheroid shrinkage or a complete spheroid collapse in several experiments. The BYL719/everolimus combination was the most effective treatment we have ever tested in PCC spheroids.

Everolimus has been approved for the treatment of NETs in many countries (65-67). Similarly to PCC/PGL with increased PI3K/AKT/mTORC1 activation (68), gastroenteropancreatic NETs also show frequent PI3K/AKT/mTORC1 over-activation (69,70). However, everolimus alone showed disappointing results in a small PCC/PGL patient study (20). Compensatory IRS-1/PI3K/AKT dis-inhibition/activation in response to mTORC1/p70S6K inhibition is the known short-term mechanism of everolimus resistance (71-75). Indeed, we found strong everolimus-induced PI3K/AKT activation in PCC cell lines and human primary cultures. In different NET cell lines the PI3Kα inhibitor BYL719 showed synergism with everolimus at clinically relevant doses (24,76) and overcame long-term everolimus resistance in human pancreatic NET cells (24). In a breast cancer model, everolimus also acted synergistically with BYL719, and delayed the development of resistance to BYL719 *in vitro* and *in vivo* (22). Consistently, we showed in our murine PCC cell lines and two different human PCC cultures that addition of BYL719 attenuated everolimus-induced AKT activation, which may essentially contribute to the synergism of both drugs. As also observed in human NET cells (24,76), BYL719/everolimus combination treatment led to synergistic inhibition of GSK3 in PCC cell lines – possibly as a consequence of IRS-1 up-regulation. IRS-1 has previously been shown to inhibit GSK3 via different signaling pathways (61,77,78), and GSK3 inhibition has shown anti-tumor potential in human NET cell lines (63).

In our murine cell lines, the BYL719/everolimus combination induced a significant G1-phase cell cycle arrest that was more prominent than in each single-drug treatment. Consistently, the BYL719/everolimus combination led to cyclin D1/D3 down-regulation in PCC cell lines and human primary cultures.

In contrast to other PI3K inhibitors, such as NVP-BEZ235 or BKM120, BYL719 is most likely to become clinically available. The phase III approval study SOLAR-1 evaluating BYL719 (alpelisib) in metastatic breast cancer has reached its final endpoints (23). Another phase IB trial is evaluating the safety of BYL719 (alpelisib) plus everolimus in advanced breast, renal cell and pancreatic cancer, including pancreatic NETs (NCT02077933).

Sunitinib is being evaluated in the first randomized, prospective, placebo-controlled clinical phase II trial in PCC/PGL (FIRST-MAPPP, NCT01371202), which has completed recruitment. A synergistic effect of sunitinib and everolimus was shown in MPC/MTT cell lines at doses exceeding clinical relevance, but not in human primary cultures. This may be in part due to additional anti-angiogenic activity of sunitinib *in vivo*, which cannot be mimicked by cell culture. However, BYL719/everolimus combination treatment seems to be more promising, as compared to sunitinib/everolimus *in vitro*. Nevertheless, one case in the literature notes an *SDHB*-mutated patient who received the mTORC1 inhibitor rapamycin in combination with sunitinib and experienced long-term disease control (21).

The combination of niraparib with temozolomide was synergistic in the MTT cells, although not in human primary cultures. PARP inhibition by niraparib suppresses DNA repair, and sensitizes tumors to alkylating DNA-damaging agents (14,79,80) thus synergizing with temozolomide in the murine PCC cell lines. Consistent with this, in an allograft PCC mouse model, a PARP inhibitor sensitized PCCs to temozolomide (15). However, temozolomide showed an absence of efficacy in human primary cultures, while niraparib and also entinostat were effective in primary cultures. This implicates fundamental differences of drug effects between murine cell lines and human primary cultures, rendering additional confirmatory drug testing in human primary cultures even more important.

Cabozantinib showed significant efficacy in PCC cell lines and human primary cultures at clinically relevant doses, but no synergism with everolimus. The PCC cell lines and human primary cultures displayed a weaker response to cabozantinib alone, as compared to everolimus/BYL719 combination treatment. Our data suggest that dual PI3K/mTORC1 inhibition might be more effective at lower doses with less toxicity. As a next step, we will investigate the most promising combination of everolimus/BYL719 *in vivo* in a suitable PCC allograft model.

The success of the different molecular-targeted therapies alone and in combination essentially depends on the individual molecular aberrations of each tumor, as shown in other tumor types (81). For example, the tumors from patients 2 and 3 are both associated with *NF1* mutations leading to MEK/RAS/ERK and mTORC1 over-activation (82-84). Accordingly, both tumor cultures responded well to both mTORC1 and PI3Kα inhibition by everolimus and BYL719, respectively, and especially to the combination, with attenuation of everolimus-induced AKT activation by BYL719. This suggests that amongst others *NF1*-mutated tumors – frequently present amongst sporadic PCCs (85) – should respond to these targeted drugs. In the PGL of patient 7, who had an unusual metastatic phenotype, no disease-causing variants were identified in any of the known PCC/PGL susceptibility genes; however, a VUS in *TET1*, a DNA demethylase, was found, which presents a potential candidate gene that needs further investigation in the future.

4.1 Conclusions

We have established a method to investigate molecular-targeted agents in human PCC primary cultures of individual patient tumors and we have correlated drug efficacy with signaling pathway alterations. The established protocol for *ex vivo* treatment of human PCC/PGL primary cultures with different molecular-targeted drugs allows screening for appropriate treatment approaches for each individual patient. In addition, we identified dual mTORC1/PI3Kα inhibition by the everolimus/BYL719 combination treatment as clinically

relevant, highly effective synergistic targeted therapy in all the PCC models investigated, including human tumor cultures.

Supplementary data

https://EMDS-NAS.quickconnect.to/d/s/496975158882345550/sUrm8NYh5szKPD5NacKzaoXM18OrpRiV-TyKA5VWc5QY_

Acknowledgements
The authors thank Susanne Schmid (study nurse) for her excellent work. The excellent technical assistance of Isabel Poser and Daniela Stanke is greatly acknowledged.

Funding

This work was funded by Deutsche Forschungsgemeinschaft (DFG) within the CRC/Transregio 205/1 "The Adrenal: Central Relay in Health and Disease" to NB, BK, CGZ, MF, FB, SRB, GE and MR and it was, in part, supported by the Intramural Research Program of the NIH, NICHD.

Deutsche Forschungsgemeinschaft http://dx.doi.org/10.13039/501100001659, CRC/Transregio 205/1, Nicole Bechmann; Eunice Kennedy Shriver National Institute of Child Health and Human Development http://dx.doi.org/10.13039/100009633, Karel Pacak

Correspondence to: Dr. med. Svenja Nölting. Med. Klinik und Poliklinik IV. Klinikum der Universität München. Ziemssenstraße 1. 80336 München. Email: svenja.noelting@med.uni-muenchen.de

Conflicts of interest statement
The authors have no conflict of interest that could be perceived as prejudicing the impartiality of the research reported. ABG has received research funding from AAA, and lecture fees from Ipsen, Roche and HRA Pharma. CJA has received research contracts from Ipsen, Novartis, and ITM Solucin, lecture honorarium from Ipsen, Novartis, and Falk Foundation, and advisory board honorarium from Novartis. SN has received research contracts from Novartis and lecture fees from Ipsen.

DATA AVAILABILITY
All data generated or analyzed during this study are included in this published article or in the data repositories listed in References.

References

1. Remine WH, Chong GC, Van Heerden JA, Sheps SG, Harrison EG, Jr. Current management of pheochromocytoma. Ann Surg 1974; 179:740-748
2. Proye CA, Vix M, Jansson S, Tisell LE, Dralle H, Hiller W. "The" pheochromocytoma: a benign, intra-adrenal, hypertensive, sporadic unilateral tumor. Does it exist? World J Surg 1994; 18:467-472
3. Goldstein RE, O'Neill JA, Jr., Holcomb GW, 3rd, Morgan WM, 3rd, Neblett WW, 3rd, Oates JA, Brown N, Nadeau J, Smith B, Page DL, Abumrad NN, Scott HW, Jr. Clinical experience over 48 years with pheochromocytoma. Ann Surg 1999; 229:755-764; discussion 764-756
4. Mannelli M, Ianni L, Cilotti A, Conti A. Pheochromocytoma in Italy: a multicentric retrospective study. Eur J Endocrinol 1999; 141:619-624
5. John H, Ziegler WH, Hauri D, Jaeger P. Pheochromocytomas: can malignant potential be predicted? Urology 1999; 53:679-683

6. Edstrom Elder E, Hjelm Skog AL, Hoog A, Hamberger B. The management of benign and malignant pheochromocytoma and abdominal paraganglioma. Eur J Surg Oncol 2003; 29:278-283
7. Amar L, Servais A, Gimenez-Roqueplo AP, Zinzindohoue F, Chatellier G, Plouin PF. Year of diagnosis, features at presentation, and risk of recurrence in patients with pheochromocytoma or secreting paraganglioma. J Clin Endocrinol Metab 2005; 90:2110-2116
8. Feng F, Zhu Y, Wang X, Wu Y, Zhou W, Jin X, Zhang R, Sun F, Kasoma Z, Shen Z. Predictive factors for malignant pheochromocytoma: analysis of 136 patients. J Urol 2011; 185:1583-1590
9. Park J, Song C, Park M, Yoo S, Park SJ, Hong S, Hong B, Kim CS, Ahn H. Predictive characteristics of malignant pheochromocytoma. Korean J Urol 2011; 52:241-246
10. Hamidi O, Young WF, Jr., Gruber L, Smestad J, Yan Q, Ponce OJ, Prokop L, Murad MH, Bancos I. Outcomes of patients with metastatic phaeochromocytoma and paraganglioma: A systematic review and meta-analysis. Clin Endocrinol (Oxf) 2017; 87:440-450
11. Mak I, Hayes AR, Khoo B, Grossman A. Peptide Receptor Radionuclide Therapy as a Novel Treatment for Metastatic and Invasive Phaeochromocytoma and Paraganglioma. Neuroendocrinology 2019;
12. Nölting S, Grossman A, Pacak K. Metastatic Phaeochromocytoma: Spinning Towards More Promising Treatment Options. Exp Clin Endocrinol Diabetes 2018;
13. Ray Chaudhuri A, Nussenzweig A. The multifaceted roles of PARP1 in DNA repair and chromatin remodelling. Nat Rev Mol Cell Biol 2017; 18:610-621
14. de Murcia JM, Niedergang C, Trucco C, Ricoul M, Dutrillaux B, Mark M, Oliver FJ, Masson M, Dierich A, LeMeur M, Walztinger C, Chambon P, de Murcia G. Requirement of poly(ADP-ribose) polymerase in recovery from DNA damage in mice and in cells. Proc Natl Acad Sci U S A 1997; 94:7303-7307
15. Pang Y, Lu Y, Caisova V, Liu Y, Bullova P, Huynh TT, Zhou Y, Yu D, Frysak Z, Hartmann I, Taieb D, Pacak K, Yang C, Yang C. Targeting NAD+/PARP DNA repair pathway as a novel therapeutic approach to SDHB-mutated cluster I pheochromocytoma and paraganglioma. Clin Cancer Res 2018;
16. Koumarianou A, Kaltsas G, Kulke MH, Oberg K, Strosberg JR, Spada F, Galdy S, Barberis M, Fumagalli C, Berruti A, Fazio N. Temozolomide in Advanced Neuroendocrine Neoplasms: Pharmacological and Clinical Aspects. Neuroendocrinology 2015; 101:274-288
17. Luchetti A, Walsh D, Rodger F, Clark G, Martin T, Irving R, Sanna M, Yao M, Robledo M, Neumann HP, Woodward ER, Latif F, Abbs S, Martin H, Maher ER. Profiling of somatic mutations in phaeochromocytoma and paraganglioma by targeted next generation sequencing analysis. Int J Endocrinol 2015; 2015:138573
18. Burnichon N, Vescovo L, Amar L, Libe R, De RA, Venisse A, Jouanno E, Laurendeau I, Parfait B, Bertherat J, Plouin PF, Jeunemaitre X, Favier J, Gimenez-Roqueplo AP. Integrative genomic analysis reveals somatic mutations in pheochromocytoma and paraganglioma. Human Molecular Genetics 2011;
19. Jochmanova I, Pacak K. Genomic Landscape of Pheochromocytoma and Paraganglioma. Trends Cancer 2018; 4:6-9
20. Druce MR, Kaltsas GA, Fraenkel M, Gross DJ, Grossman AB. Novel and evolving therapies in the treatment of malignant phaeochromocytoma: experience with the mTOR inhibitor everolimus (RAD001). Hormone and metabolic research = Hormon- und Stoffwechselforschung = Hormones et metabolisme 2009; 41:697–702
21. Ayala-Ramirez M, Chougnet CN, Habra MA, Palmer JL, Leboulleux S, Cabanillas ME, Caramella C, Anderson P, Al Ghuzlan A, Waguespack SG, Deandreis D, Baudin E,

Jimenez C. Treatment with sunitinib for patients with progressive metastatic pheochromocytomas and sympathetic paragangliomas. The Journal of clinical endocrinology and metabolism 2012; 97:4040–4050

22. Elkabets M, Vora S, Juric D, Morse N, Mino-Kenudson M, Muranen T, Tao J, Campos AB, Rodon J, Ibrahim YH, Serra V, Rodrik-Outmezguine V, Hazra S, Singh S, Kim P, Quadt C, Liu M, Huang A, Rosen N, Engelman JA, Scaltriti M, Baselga J. mTORC1 inhibition is required for sensitivity to PI3K p110α inhibitors in PIK3CA-mutant breast cancer. Science translational medicine 2013; 5:196ra199

23. Andre F, Ciruelos E, Rubovszky G, Campone M, Loibl S, Rugo HS, Iwata H, Conte P, Mayer IA, Kaufman B, Yamashita T, Lu YS, Inoue K, Takahashi M, Papai Z, Longin AS, Mills D, Wilke C, Hirawat S, Juric D, Group S-S, the S-SG. Alpelisib for PIK3CA-Mutated, Hormone Receptor-Positive Advanced Breast Cancer. N Engl J Med 2019; 380:1929-1940

24. Aristizabal Prada ET, Spoettl G, Maurer J, Lauseker M, Koziolek E, Schrader J, Grossman AB, Pacak K, Beuschlein F, Auernhammer CJ, Nölting S. The role of GSK3 and its reversal with GSK3 antagonism in everolimus resistance. Endocr Relat Cancer 2018;

25. Powers JF, Evinger MJ, Tsokas P, Bedri S, Alroy J, Shahsavari M, Tischler AS. Pheochromocytoma cell lines from heterozygous neurofibromatosis knockout mice. Cell and tissue research 2000; 302:309–320

26. Martiniova L, Lai EW, Elkahloun AG, Abu-Asab M, Wickremasinghe A, Solis DC, Perera SM, Huynh T-T, Lubensky IA, Tischler AS, Kvetnansky R, Alesci S, Morris JC, Pacak K. Characterization of an animal model of aggressive metastatic pheochromocytoma linked to a specific gene signature. Clinical & experimental metastasis 2009; 26:239–250

27. Nölting S, Garcia E, Alusi G, Giubellino A, Pacak K, Korbonits M, Grossman AB. Combined blockade of signalling pathways shows marked anti-tumour potential in phaeochromocytoma cell lines. Journal of molecular endocrinology 2012; 49:79–96

28. Almeida JL, Hill CR, Cole KD. Mouse cell line authentication. Cytotechnology 2014; 66:133–147

29. Letouze E, Martinelli C, Loriot C, Burnichon N, Abermil N, Ottolenghi C, Janin M, Menara M, Nguyen AT, Benit P, Buffet A, Marcaillou C, Bertherat J, Amar L, Rustin P, De Reynies A, Gimenez-Roqueplo AP, Favier J. SDH mutations establish a hypermethylator phenotype in paraganglioma. Cancer Cell 2013; 23:739-752

30. Budde K, Zonnenberg BA, Frost M, Cheung W, Urva S, Brechenmacher T, Stein K, Chen D, Kingswood JC, Bissler JJ. Pharmacokinetics and pharmacodynamics of everolimus in patients with renal angiomyolipoma and tuberous sclerosis complex or lymphangioleiomyomatosis. British journal of clinical pharmacology 2016; 81:958–970

31. Buck SSd, Jakab A, Boehm M, Bootle D, Juric D, Quadt C, Goggin TK. Population pharmacokinetics and pharmacodynamics of BYL719, a phosphoinositide 3-kinase antagonist, in adult patients with advanced solid malignancies. British journal of clinical pharmacology 2014; 78:543–555

32. Faivre S, Delbaldo C, Vera K, Robert C, Lozahic S, Lassau N, Bello C, Deprimo S, Brega N, Massimini G, Armand J-P, Scigalla P, Raymond E. Safety, pharmacokinetic, and antitumor activity of SU11248, a novel oral multitarget tyrosine kinase inhibitor, in patients with cancer. Journal of clinical oncology : official journal of the American Society of Clinical Oncology 2006; 24:25–35

33. Miles D, Jumbe NL, Lacy S, Nguyen L. Population Pharmacokinetic Model of Cabozantinib in Patients with Medullary Thyroid Carcinoma and Its Application to an Exposure-Response Analysis. Clinical pharmacokinetics 2016; 55:93–105

34. Feoktistova M, Geserick P, Leverkus M. Crystal Violet Assay for Determining Viability of Cultured Cells. Cold Spring Harbor protocols 2016; 2016:pdb.prot087379

35. Bechmann N, Ehrlich H, Eisenhofer G, Ehrlich A, Meschke S, Ziegler CG, Bornstein SR. Anti-Tumorigenic and Anti-Metastatic Activity of the Sponge-Derived Marine Drugs Aeroplysinin-1 and Isofistularin-3 against Pheochromocytoma In Vitro. Marine drugs 2018; 16
36. Bechmann N, Poser I, Seifert V, Greunke C, Ullrich M, Qin N, Walch A, Peitzsch M, Robledo M, Pacak K, Pietzsch J, Richter S, Eisenhofer G. Impact of Extrinsic and Intrinsic Hypoxia on Catecholamine Biosynthesis in Absence or Presence of Hif2alpha in Pheochromocytoma Cells. Cancers (Basel) 2019; 11
37. Reuther C, Heinzle V, Spampatti M, Vlotides G, Toni Ed, Spöttl G, Maurer J, Nölting S, Göke B, Auernhammer CJ. Cabozantinib and Tivantinib, but Not INC280, Induce Antiproliferative and Antimigratory Effects in Human Neuroendocrine Tumor Cells in vitro: Evidence for 'Off-Target' Effects Not Mediated by c-Met Inhibition. Neuroendocrinology 2016; 103:383–401
38. RRID:AB_2315049, https://scicrunch.org/resolver/RRID:AB_2315049.
39. RRID: AB_329827, https://scicrunch.org/resolver/RRID:AB_329827.
40. RRID: AB_330947, https://scicrunch.org/resolver/RRID:AB_330947.
41. RRID:AB_2097841, https://scicrunch.org/resolver/RRID:AB_2097841,.
42. RRID: AB_10695803, https://scicrunch.org/resolver/RRID:AB_10695803,.
43. RRID:AB_2259616, https://scicrunch.org/resolver/RRID:AB_2259616.
44. RRID:AB_2070801, https://scicrunch.org/resolver/RRID:AB_2070801.
45. RRID:AB_330944, https://scicrunch.org/resolver/RRID:AB_330944.
46. RRID:AB_390722, https://scicrunch.org/resolver/RRID:AB_390722,.
47. RRID:AB_10694233, https://scicrunch.org/resolver/RRID:AB_10694233.
48. RRID:AB_331355, https://scicrunch.org/resolver/RRID:AB_331355.
49. RRID: AB_329830, https://scicrunch.org/resolver/RRID:AB_329830.
50. RRID:AB_10547140, https://scicrunch.org/resolver/RRID:AB_10547140.
51. RRID:AB_2074795, https://scicrunch.org/resolver/RRID:AB_2074795.
52. RRID:AB_2080320, https://scicrunch.org/resolver/RRID:AB_2080320.
53. RRID:AB_2536328, https://scicrunch.org/resolver/RRID:AB_2536328.
54. RRID:AB_2533767, https://scicrunch.org/resolver/RRID:AB_2533767.
55. RRID:AB_476744, https://scicrunch.org/resolver/RRID:AB_476744
56. RRID:AB_95187, https://scicrunch.org/resolver/RRID:AB_95187
57. Gieldon L, William D, Hackmann K, Jahn W, Jahn A, Wagner J, Rump A, Bechmann N, Nolting S, Knosel T, Gudziol V, Constantinescu G, Masjkur J, Beuschlein F, Timmers HJ, Canu L, Pacak K, Robledo M, Aust D, Schrock E, Eisenhofer G, Richter S, Klink B. Optimizing Genetic Workup in Pheochromocytoma and Paraganglioma by Integrating Diagnostic and Research Approaches. Cancers (Basel) 2019; 11
58. https://EMDS-NAS.quickconnect.to/d/s/49697515888234555O/sUrm8NYh5szKPD5NacKzaoXM18OrpRiV-TyKA5VWc5QY_
59. Rump A, Benet-Pages A, Schubert S, Kuhlmann JD, Janavicius R, Machackova E, Foretova L, Kleibl Z, Lhota F, Zemankova P, Betcheva-Krajcir E, Mackenroth L, Hackmann K, Lehmann J, Nissen A, DiDonato N, Opitz R, Thiele H, Kast K, Wimberger P, Holinski-Feder E, Emmert S, Schrock E, Klink B. Identification and Functional Testing of ERCC2 Mutations in a Multi-national Cohort of Patients with Familial Breast- and Ovarian Cancer. PLoS Genet 2016; 12:e1006248
60. Slinker BK. The statistics of synergism. J Mol Cell Cardiol 1998; 30:723-731
61. Maurer U, Preiss F, Brauns-Schubert P, Schlicher L, Charvet C. GSK-3 - at the crossroads of cell death and survival. J Cell Sci 2014; 127:1369-1378

62. Pirola L, Bonnafous S, Johnston AM, Chaussade C, Portis F, van Obberghen E. Phosphoinositide 3-kinase-mediated reduction of insulin receptor substrate-1/2 protein expression via different mechanisms contributes to the insulin-induced desensitization of its signaling pathways in L6 muscle cells. The Journal of biological chemistry 2003; 278:15641–15651
63. Aristizabal Prada ET, Weis C, Orth M, Lauseker M, Spöttl G, Maurer J, Grabowski P, Grossman A, Auernhammer CJ, Nölting S. GSK3α/β: A Novel Therapeutic Target for Neuroendocrine Tumors. Neuroendocrinology 2018; 106:335–351
64. Timmers HJ, Kozupa A, Eisenhofer G, Raygada M, Adams KT, Solis D, Lenders JW, Pacak K. Clinical presentations, biochemical phenotypes, and genotype-phenotype correlations in patients with succinate dehydrogenase subunit B-associated pheochromocytomas and paragangliomas. J Clin Endocrinol Metab 2007; 92:779-786
65. Pavel ME, Hainsworth JD, Baudin E, Peeters M, Horsch D, Winkler RE, Klimovsky J, Lebwohl D, Jehl V, Wolin EM, Oberg K, van Cutsem E, Yao JC. Everolimus plus octreotide long-acting repeatable for the treatment of advanced neuroendocrine tumours associated with carcinoid syndrome (RADIANT-2): a randomised, placebo-controlled, phase 3 study. Lancet (London, England) 2011; 378:2005–2012
66. Yao JC, Shah MH, Ito T, Bohas CL, Wolin EM, van Cutsem E, Hobday TJ, Okusaka T, Capdevila J, de Vries EGE, Tomassetti P, Pavel ME, Hoosen S, Haas T, Lincy J, Lebwohl D, Oberg K. Everolimus for advanced pancreatic neuroendocrine tumors. The New England journal of medicine 2011; 364:514–523
67. Yao JC, Fazio N, Singh S, Buzzoni R, Carnaghi C, Wolin E, Tomasek J, Raderer M, Lahner H, Voi M, Pacaud LB, Rouyrre N, Sachs C, Valle JW, Fave GD, van Cutsem E, Tesselaar M, Shimada Y, Oh D-Y, Strosberg J, Kulke MH, Pavel ME. Everolimus for the treatment of advanced, non-functional neuroendocrine tumours of the lung or gastrointestinal tract (RADIANT-4): a randomised, placebo-controlled, phase 3 study. Lancet (London, England) 2016; 387:968–977
68. Fassnacht M, Weismann D, Ebert S, Adam P, Zink M, Beuschlein F, Hahner S, Allolio B. AKT is highly phosphorylated in pheochromocytomas but not in benign adrenocortical tumors. J Clin Endocrinol Metab 2005; 90:4366-4370
69. Briest F, Grabowski P. PI3K-AKT-mTOR-signaling and beyond: the complex network in gastroenteropancreatic neuroendocrine neoplasms. Theranostics 2014; 4:336-365
70. Pavel M. Translation of molecular pathways into clinical trials of neuroendocrine tumors. Neuroendocrinology 2013; 97:99-112
71. O'Reilly KE, Rojo F, She QB, Solit D, Mills GB, Smith D, Lane H, Hofmann F, Hicklin DJ, Ludwig DL, Baselga J, Rosen N. mTOR inhibition induces upstream receptor tyrosine kinase signaling and activates Akt. Cancer Research 2006; 66:1500-1508
72. Carracedo A, Ma L, Teruya-Feldstein J, Rojo F, Salmena L, Alimonti A, Egia A, Sasaki AT, Thomas G, Kozma SC, Papa A, Nardella C, Cantley LC, Baselga J, Pandolfi PP. Inhibition of mTORC1 leads to MAPK pathway activation through a PI3K-dependent feedback loop in human cancer. Journal of Clinical Investigation 2008; 118:3065-3074
73. Zitzmann K, Ruden J, Brand S, Goke B, Lichtl J, Spottl G, Auernhammer CJ. Compensatory activation of Akt in response to mTOR and Raf inhibitors - a rationale for dual-targeted therapy approaches in neuroendocrine tumor disease. Cancer Letters 2010; 295:100-109
74. Svejda B, Kidd M, Kazberouk A, Lawrence B, Pfragner R, Modlin IM. Limitations in small intestinal neuroendocrine tumor therapy by mTor kinase inhibition reflect growth factor-mediated PI3K feedback loop activation via ERK1/2 and AKT. Cancer 2011; 117:4141-4154

75. Passacantilli I, Capurso G, Archibugi L, Calabretta S, Caldarola S, Loreni F, Delle Fave G, Sette C. Combined therapy with RAD001 e BEZ235 overcomes resistance of PET immortalized cell lines to mTOR inhibition. Oncotarget 2014; 5:5381-5391
76. Nölting S, Rentsch J, Freitag H, Detjen K, Briest F, Mobs M, Weissmann V, Siegmund B, Auernhammer CJ, Aristizabal Prada ET, Lauseker M, Grossman A, Exner S, Fischer C, Grotzinger C, Schrader J, Grabowski P, group GN-Zs. The selective PI3Kalpha inhibitor BYL719 as a novel therapeutic option for neuroendocrine tumors: Results from multiple cell line models. PLoS One 2017; 12:e0182852
77. Cohen P, Frame S. The renaissance of GSK3. Nat Rev Mol Cell Biol 2001; 2:769-776
78. Wada A. GSK-3 inhibitors and insulin receptor signaling in health, disease, and therapeutics. Front Biosci (Landmark Ed) 2009; 14:1558-1570
79. Genther Williams SM, Kuznicki AM, Andrade P, Dolinski BM, Elbi C, O'Hagan RC, Toniatti C. Treatment with the PARP inhibitor, niraparib, sensitizes colorectal cancer cell lines to irinotecan regardless of MSI/MSS status. Cancer Cell Int 2015; 15:14
80. Kanjanapan Y, Lheureux S, Oza AM. Niraparib for the treatment of ovarian cancer. Expert Opin Pharmacother 2017; 18:631-640
81. Hagemann IS, Devarakonda S, Lockwood CM, Spencer DH, Guebert K, Bredemeyer AJ, Al-Kateb H, Nguyen TT, Duncavage EJ, Cottrell CE, Kulkarni S, Nagarajan R, Seibert K, Baggstrom M, Waqar SN, Pfeifer JD, Morgensztern D, Govindan R. Clinical next-generation sequencing in patients with non–small cell lung cancer. Cancer 2015; 121:631–639
82. Johannessen CM, Reczek EE, James MF, Brems H, Legius E, Cichowski K. The NF1 tumor suppressor critically regulates TSC2 and mTOR 1. Proceedings of the National Academy of Sciences of the USA 2005; 102:8573-8578
83. Johannessen CM, Johnson BW, Williams SM, Chan AW, Reczek EE, Lynch RC, Rioth MJ, McClatchey A, Ryeom S, Cichowski K. TORC1 is essential for NF1-associated malignancies 1. Current Biology 2008; 18:56-62
84. Martin GA, Viskochil D, Bollag G, McCabe PC, Crosier WJ, Haubruck H, Conroy L, Clark R, O'Connell P, Cawthon RM. The GAP-related domain of the neurofibromatosis type 1 gene product interacts with ras p21. Cell 1990; 63:843-849
85. Welander J, Soderkvist P, Gimm O. The NF1 gene: a frequent mutational target in sporadic pheochromocytomas and beyond. Endocr Relat Cancer 2013; 20:C13-17

Figure 1. Overview: **Cluster-1, -2 and -3, with molecular-targeted therapeutic options:** Cluster-1: The pseudo-hypoxic signaling cluster includes mutations in genes encoding for hypoxia-inducible factor 2-alpha (*HIF2A*), Krebs-cycle enzymes such as succinate dehydrogenase subunits (*SDHx* [*SDHA, SDHB, SDHC, SDHD*]), succinate dehydrogenase complex assembly factor-2 (*SDHAF2*), fumarate hydratase (*FH*), malate dehydrogenase 2 (*MDH2*), and isocitrate dehydrogenase (*IDH*), and including von Hippel–Lindau tumor suppressor (*VHL*) and egl-9 prolyl hydroxylase 1 and 2 (*EGLN1/2*). Cluster-2: The kinase signaling cluster comprises mutations in the rearranged-during-transfection (*RET)* proto-oncogene, neurofibromin 1 (*NF1)* tumor suppressor, *H-RAS* and *K-RAS* proto-oncogenes, transmembrane protein 127 (*TMEM127)* and Myc-associated factor X (*MAX)*. Receptor tyrosine kinases (amongst others RET, vascular endothelial cell growth factor (VEGFR), c-met) activate insulin receptor substrate 1 (IRS-1) which recruits the phosphatidylinositol-3-kinase (PI3K). PI3K activates AKT, which inhibits tuberous sclerosis proteins 1/2 (TSC1/2) leading to disinhibition/activation of the mammalian target of rapamycin (mTORC1); mTORC1 phosphorylates and activates various proteins including p70S6 kinase (p70S6K), by which p70S6 is phosphorylated. Activated p70S6 promotes cell growth, proliferation, cell survival, and leads amongst other effects to the protein synthesis of HIF-1α, which favors

angiogenesis [VEGF/platelet-derived growth factor (PDGF) transcription amongst others], invasion and metastasis under hypoxic or pseudo-hypoxic conditions. AKT also inhibits glycogen synthase kinase 3 (GSK3). Persistent activation of PI3K leads to feed-back down-regulation of IRS-1, which in turn may lead to GSK3 dis-inhibition/activation. The RAS/RAF/ERK-pathway is also activated by tyrosine kinases (amongst others RET) and activates mTORC1. *NF1* mutations lead to disinhibition/activation of RAS. *TMEM127* mutations lead to disinhibition/activation of mTORC1. The tumor suppressor MAX antagonizes Myc-dependent cell survival, proliferation and angiogenesis: mutations lead to increased cell proliferation and angiogenesis. Cluster-3: The Wnt signaling cluster comprises somatic mutations in cold shock domain containing E1 (*CSDE1*) and the mastermind like transcriptional coactivator 3 (*MAML3*) fusion genes. ⊘ Pheochromocytoma promoting loss of function mutation of a tumor suppressor gene. Pheochromocytoma promoting gain of function mutation of a proto-oncogene. ⇧ Increase/up-regulation. ⊥ Inhibition. ↘ Activation

Figure 2. Significant MPC/MTT cell viability reduction by clinically relevant doses of BYL719, everolimus and by the combination of both after 120h. The BYL719/everolimus combination treatment was statistically synergistic (@) in MPC cells and additive in MTT cells. The arithmetic means and standard deviation of at least three independent experiments are shown. Statistically significant differences in comparison to the DMSO control are shown, considering $p<0.05$ as significant (*).

Figure 3. Significant MPC/MTT cell viability reduction by sunitinib, everolimus and by the combination of both after 120h. Sunitinib/everolimus combination treatment was statistically synergistic (@) in both cell lines. The arithmetic means and standard deviation of at least three independent experiments are shown. Statistically significant differences in comparison to the DMSO control are shown, considering $p<0.05$ as significant (*).

Figure 4. Significant MPC/MTT cell viability reduction by niraparib, temozolomide and by the combination of both after 120h. The niraparib/temozolomide combination was statistically synergistic (@) in MTT cells, but not in MPC cells. Statistically significant differences in comparison to the DMSO control are shown, considering $p<0.05$ as significant (*).

Figure 5. Cell cycle analysis via FACS: Significant induction of a G1-phase cell cycle arrest in MPC cells by BYL719, everolimus or sunitinib alone and – even stronger – by the BYL719/everolimus and sunitinib/everolimus combination treatments at 24h treatment. Significant induction of a G1-phase cell cycle arrest in MTT cells by everolimus (10nM) and sunitinib (1µM/2µM) and – even stronger – by the BYL719/everolimus and sunitinib/everolimus combination treatment at 24h treatment. The arithmetic means and standard deviation of at least three independent experiments are shown. Statistically significant differences in comparison to the DMSO control are shown, considering $p<0.05$ as significant (*).

Figure 6. Mean caspase-3/-7 activity in percent ± standard deviation in MPC/MTT cell lines after 24h of incubation with different drugs. In both cell lines significant apoptosis induction was observed after BYL719 treatment alone, after tBYL719/everolimus combination treatment, and - to a lesser extent - after sunitinib/everolimus combination treatment. The arithmetic means and standard deviation of at least three independent experiments are shown. Statistically significant differences in comparison to the DMSO control are shown, considering $p<0.05$ as significant (*).

Figure 7. Western blot analysis of MPC/MTT cell lines after 24h or 48h of incubation with different drugs: Inhibition of p70S6K, S6, 4EBP1 and GSK3 signaling, attenuation of everolimus-induced AKT activation, IRS-1 up-regulation and cyclin D1/D3 down-regulation after BYL719/everolimus combination treatment. A representative blot of three independently performed experiments is shown.

Figure 8. Significant reduction of cell viability after BYL719 and everolimus treatment in immortalized mouse chromaffin wild-type (WT) and *Sdhb-/-* cells at 48h and 72h with a synergistic effect (@) of the combination in both cell lines at 72h, and a significantly stronger effect of BYL719 alone in the *Sdhb-/-* compared to the WT cells. Significant difference between WT and *Sdhb-/-* (Δ). Statistically significant differences in comparison to the DMSO control are shown, considering $p<0.05$ as significant (*).

Figure 9. Significant MPC/MTT spheroid shrinkage or complete spheroid collapse after fractionated treatment with 5µM BYL719, even stronger shrinkage, as compared to BYL719 alone, or an early complete collapse of the spheroids in several experiments after fractionated treatment with the BYL719/everolimus combination, and spheroid growth inhibition after fractionated treatment with 25nM everolimus. Spheroids were treated with different concentrations of BYL719 and everolimus after completed spheroid formation (day 4) and, in addition, on day 7, 11, and 14 (fractionated treatment). Growth was monitored over a time period of 18 days. The arithmetic means and all single values of each experiment of at least three independent experiments are shown. Statistically significant different results in comparison to the DMSO control are shown, considering $p<0.05$ as significant (*).

Figure 10. Significant reduction of human PCC primary culture viability (n=6) by clinically relevant doses of BYL719, everolimus and the combination of BYL719 plus everolimus at 72h treatment, showing a synergistic effect (@) of 5µM BYL719 plus 10nM everolimus. Moreover, a significant reduction of human PCC primary culture viability (n=6) by sunitinib and the combination of sunitinib plus everolimus is seen at 72h. Sunitinib and everolimus did not act synergistically. The arithmetic means and all single values of six human PCC cultures from six different patients are shown. Statistically significant different results in comparison to the DMSO control are shown, considering *$p<0.05$ as significant (*).

Figure 11. Significant reduction of human PCC primary culture viability (n=5) by cabozantinib, entinostat and niraparib, but not temozolomide, at 72h treatment. The arithmetic means and all single values of five human PCC primary cultures from five different patients are shown. Statistically significant different results in comparison to the DMSO control are shown, considering $p<0.05$ as significant (*).

Figure 12. Western blot analysis of the human primary cultures from patients 2, 3 and 5 after 24h of incubation with different drugs. There was strong synaptophysin expression in all primary cultures. There was strong inhibition of mTORC1/p70S6K and 4EBP1 signaling by everolimus and all combination treatments, attenuation of everolimus-induced AKT activation by the combination treatment in the primary cultures from patients 3 and 5, and down-regulation of cyclin D3, CDK1 cdc2 (patient 3), chk1 (patients 3, 5) and p53 by the combination treatment. GSK3 showed no clear differences – most likely due to suboptimal incubation times.

Table 1. Clinical and histological characteristics of the human PCC/PGL primary cultures from 7 different patients

	Age	Sex	Tumor	metastatic	Histology and criteria of	Ki-67	Next Generation

					malignancy	(%)	Sequencing (NGS) of the tumors
Patient 1	82	M	Adrenal pheochromocytoma	no	Tumor size: 1.5 cm, **capsule invasion**	1-2	No known susceptibility mutation
Patient 2	50	M	Adrenal pheochromocytoma	no	**Tumor size: 12.9 cm,** nuclear pleomorphism	1-2	*NF1* mutation
Patient 3	73	F	Adrenal pheochromocytoma	no	Tumor size: 3.9 cm, nuclear and cell pleomorphism	2	*NF1* mutation
Patient 4	26	M	Adrenal pheochromocytoma	no	Tumor size: 3.2 cm, **vascular invasion,** anisonucleosis, cell inclusions	**5**	No known susceptibility mutation
Patient 5	65	M	Adrenal pheochromocytoma	no	Tumor size: 5 cm	<1	not assessed
Patient 6	60	M	Adrenal pheochromocytoma	no	**Tumor size: 5.5 cm, capsule invasion, vascular invasion**	<1	not assessed
Patient 7	30	F	Uterus metastasis	yes	Tumor size: 5.3 cm	20	Variance of unknown significance (VUS) in *TET1*
			Lymph node metastasis	yes	Tumor size: 2.5 cm	20	

Figure 1

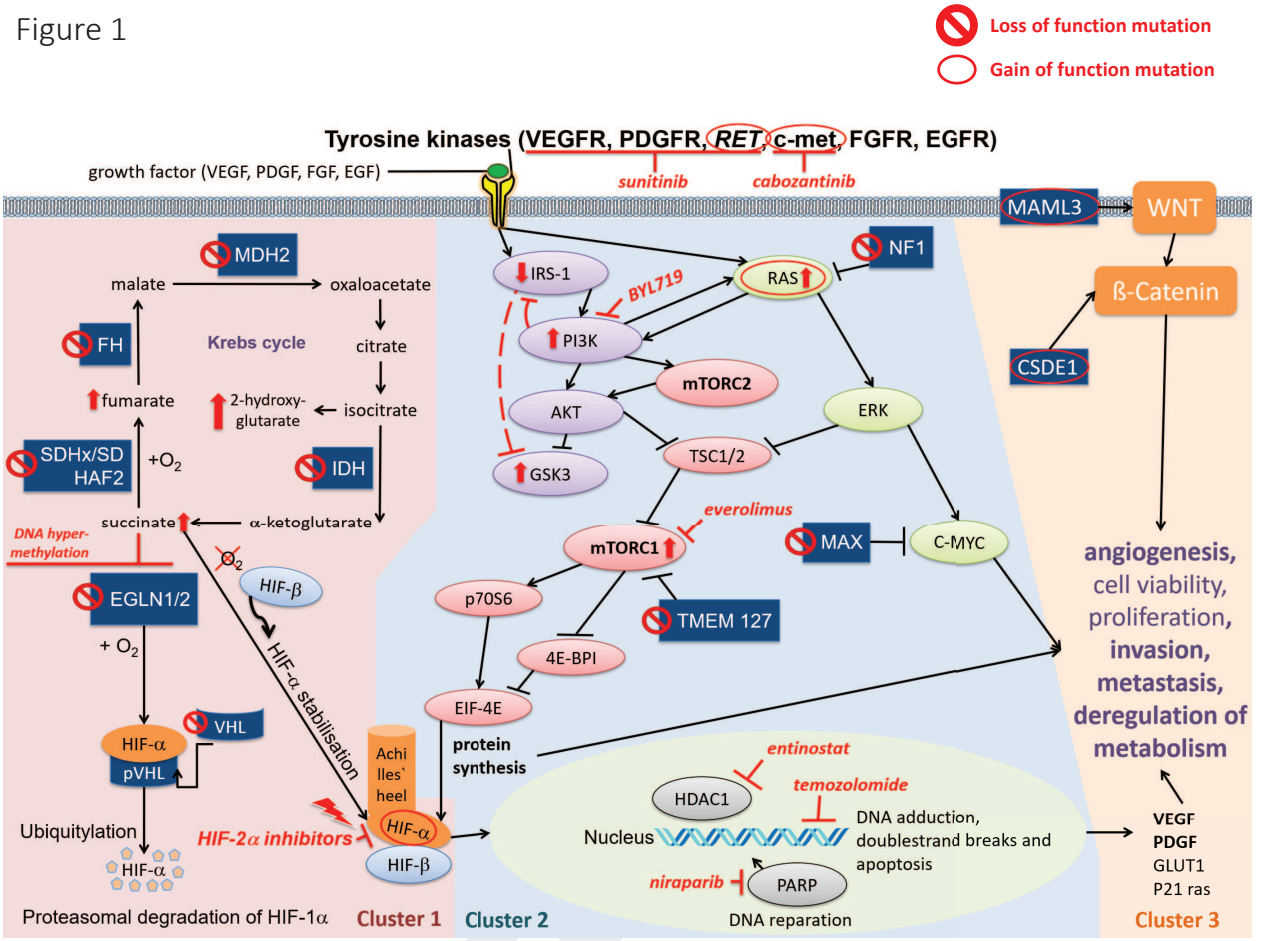

Figure 2

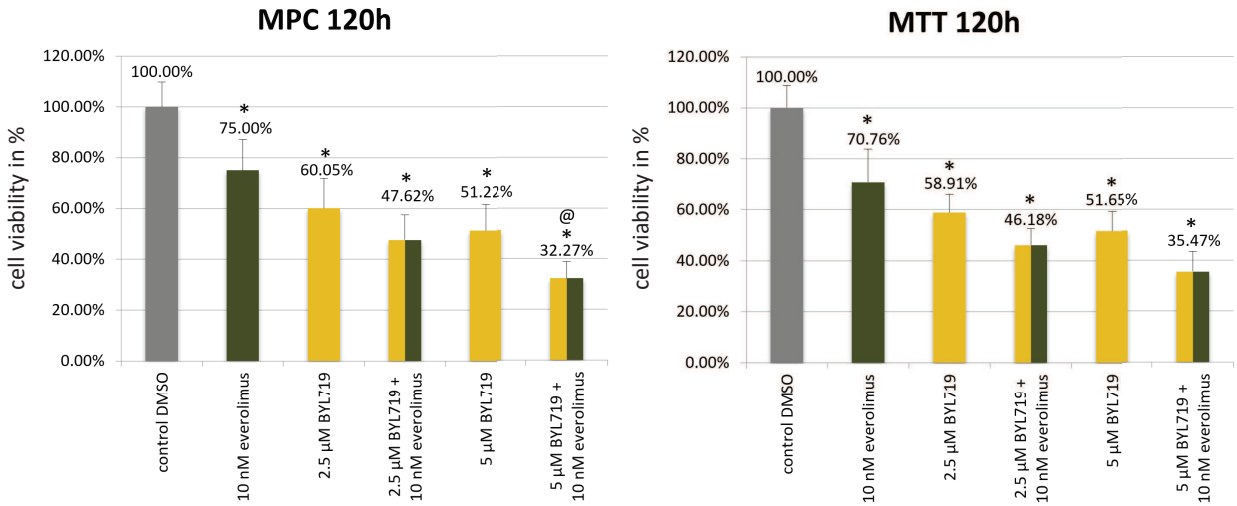

@ Synergistic effect of BYL719/everolimus in MPC cells
* Significant decrease of cell viability compared to control DMSO

Figure 3

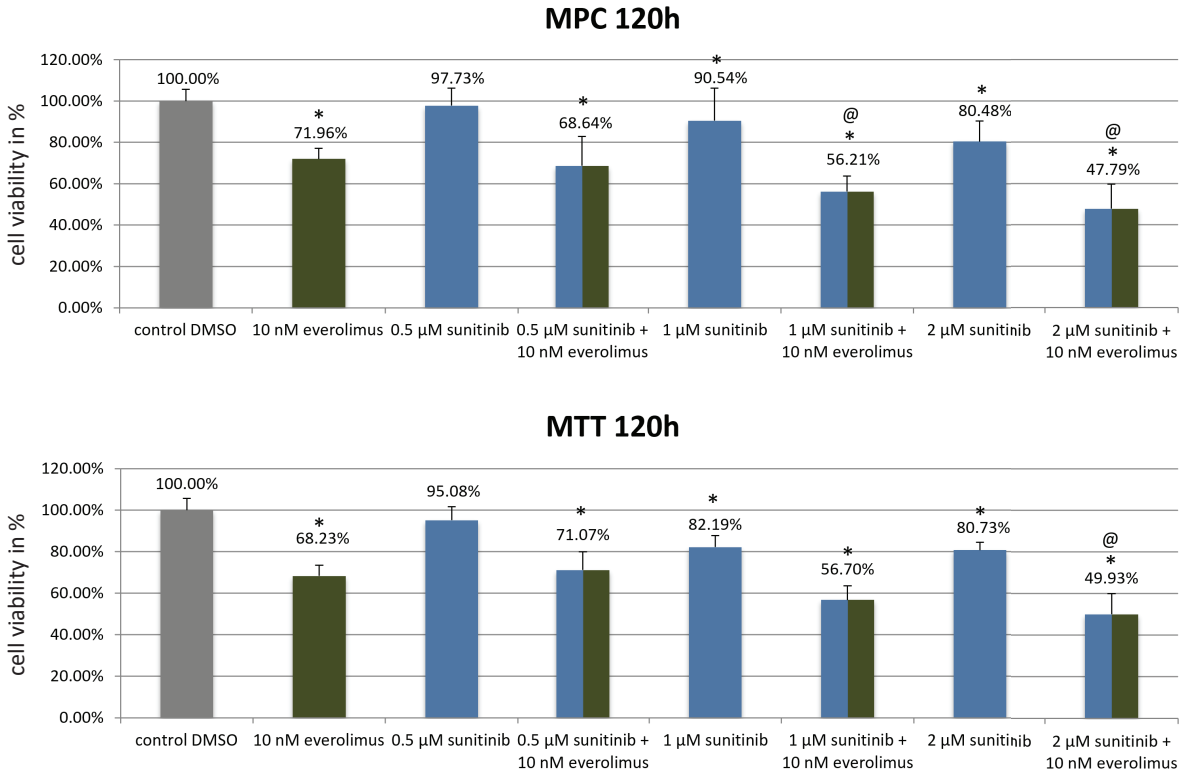

@ Synergistic effect of sunitinib/everolimus in MPC/MTT cells
* Significant decrease of cell viability compared to control DMSO

Figure 4

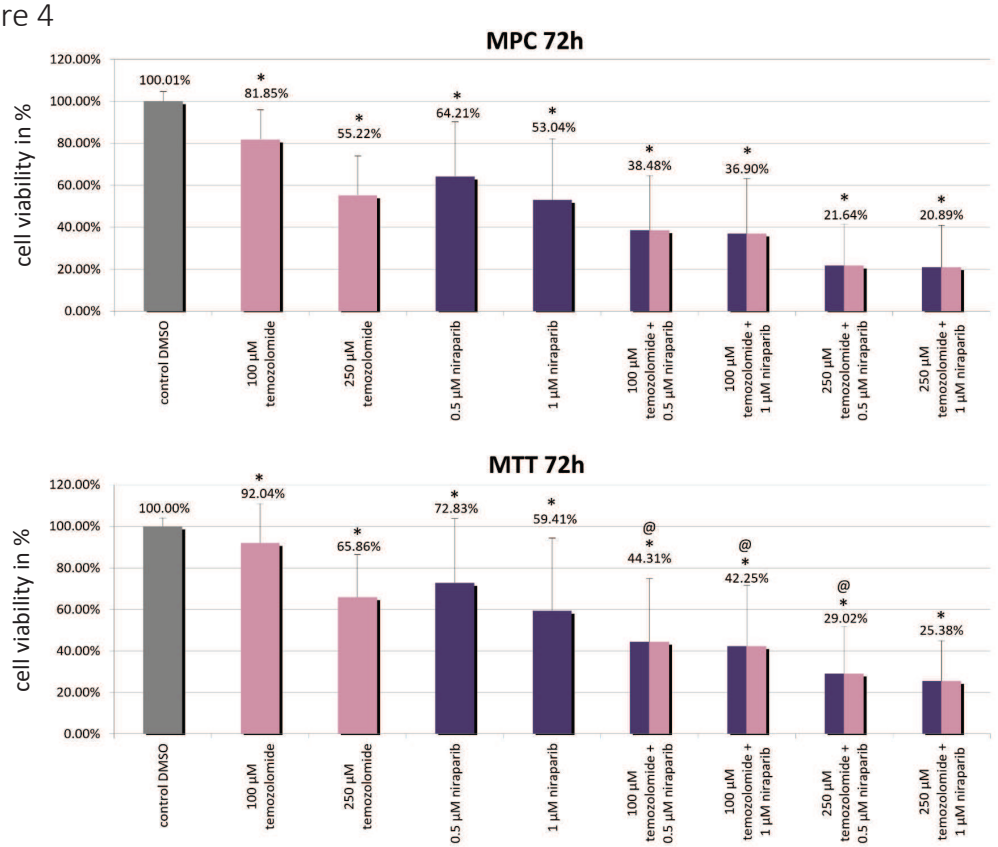

@ Synergistic effect of temozolomide/niraparib in MTT cells
* Significant decrease of cell viability compared to control DMSO

Figure 5

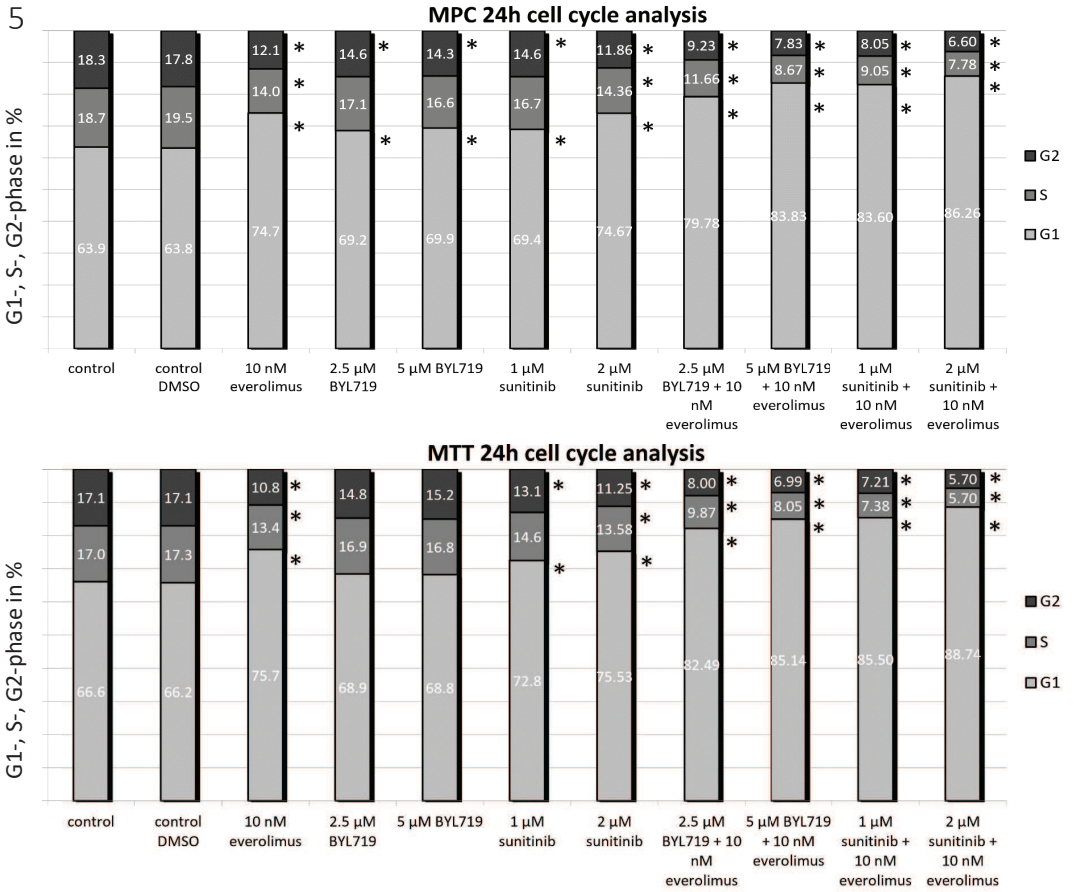

* Significant difference of the percentage of cells in the respective cell cycle phase between control DMSO and different treatments

Figure 6

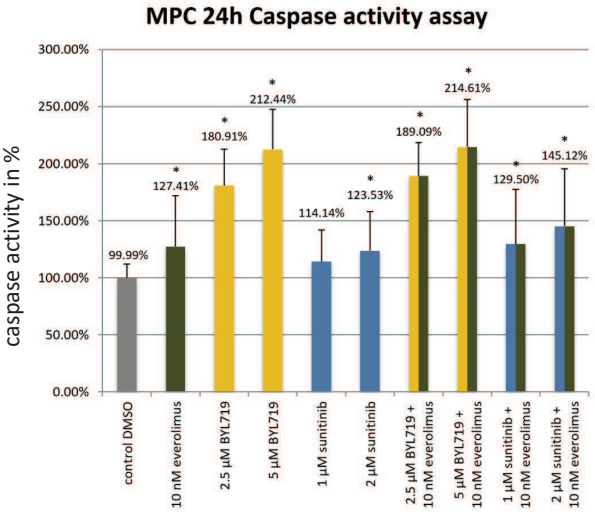

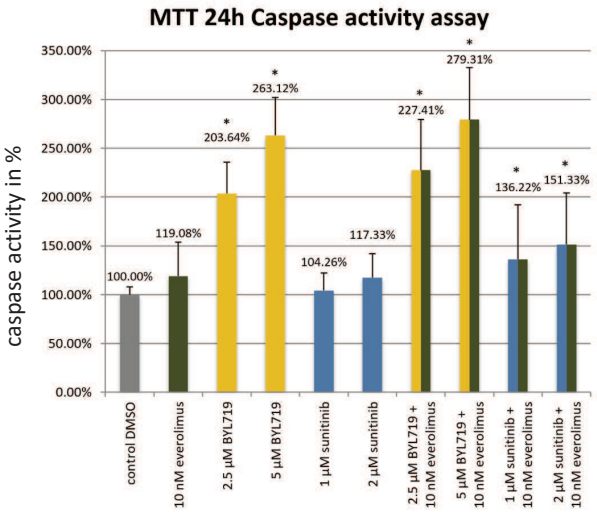

* Significant increase of caspase activity compared to control DMSO

Figure 7

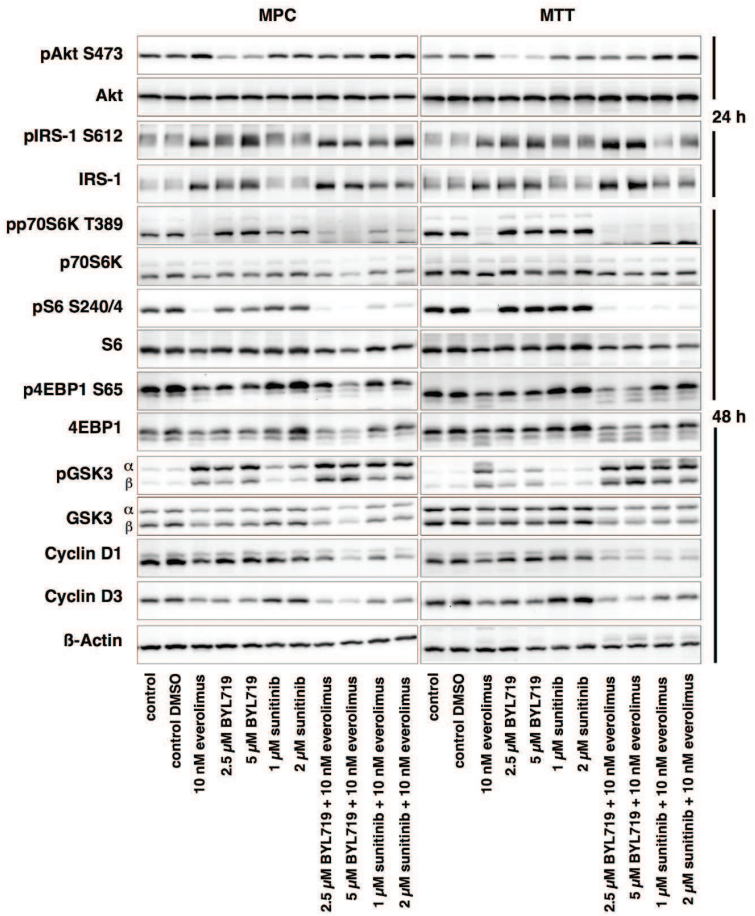

Figure 8

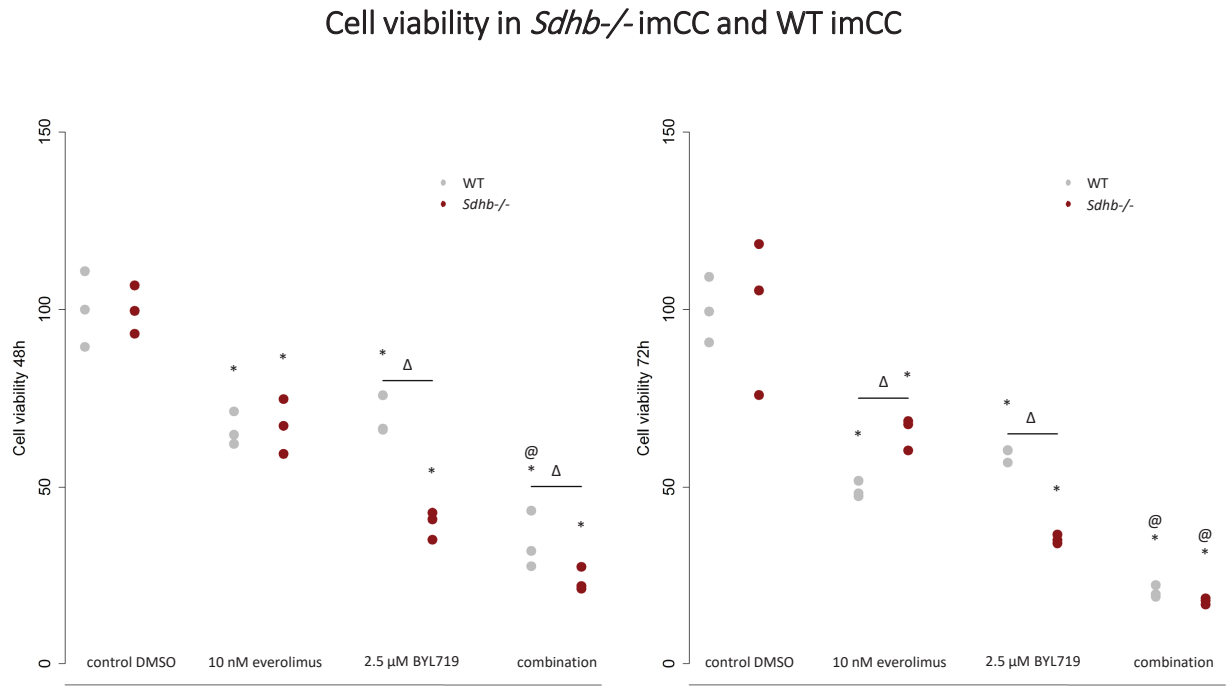

@ Synergistic effect of BYL719/everolimus
* Significant decrease of cell viability compared to control DMSO
Δ Significant difference between WT and *Sdhb-/-*

Figure 9

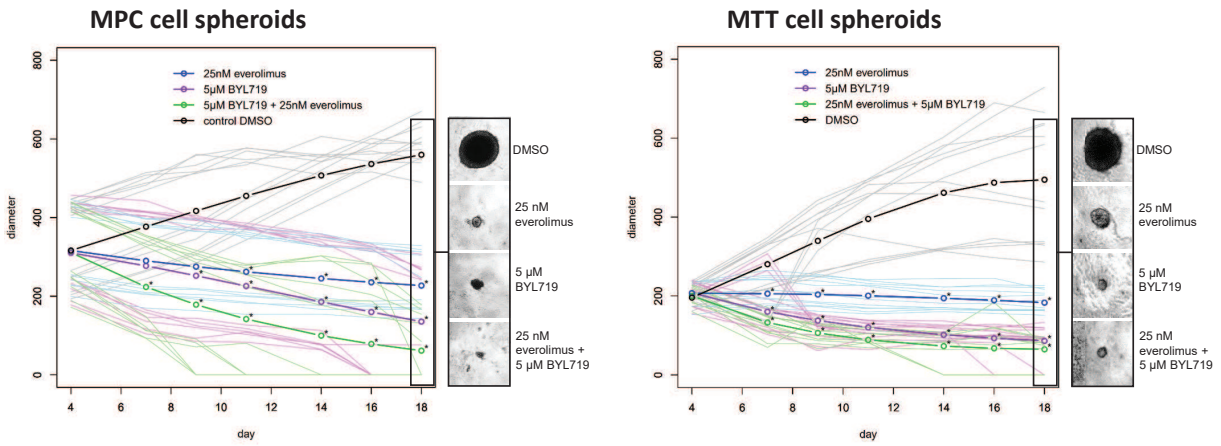

* Significant decrease of spheroid size compared to control DMSO

Figure 10

BYL719/everolimus and sunitinib/everolimus treatment in human PCC primary cultures (n=6)

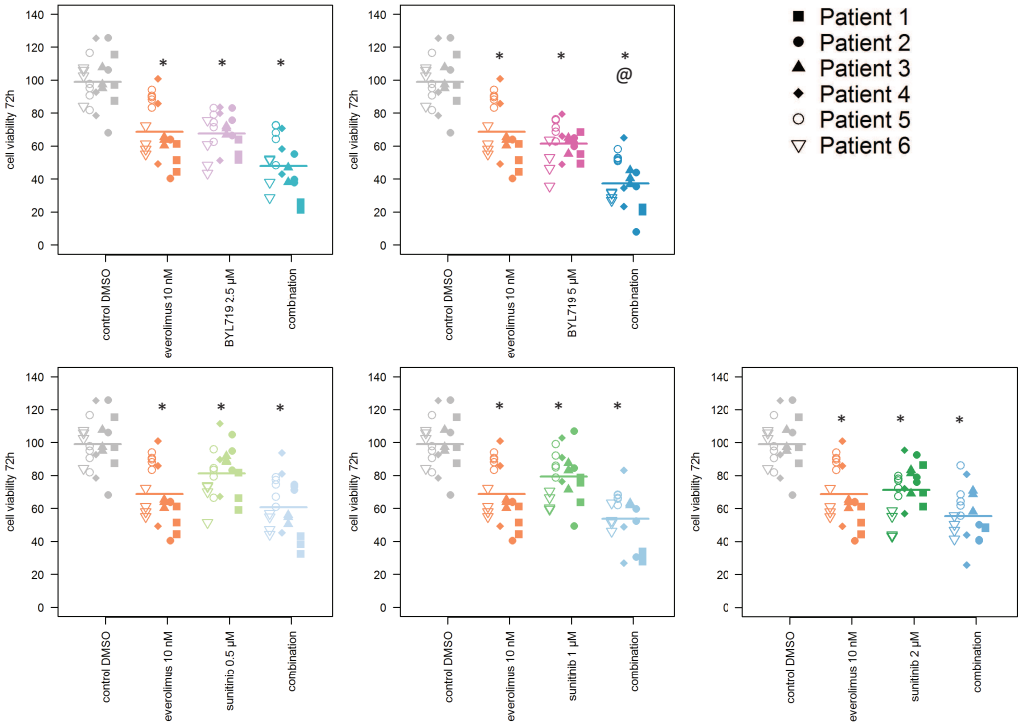

@ Synergistic effect of everolimus/BYL719 in human PCC primary cells

* Significant decrease of cell viability compared to control DMSO

Figure 11

Cabozantinib, entinostat, niraparib and temozolomide treatment in human PCC primary cultures (n=5)

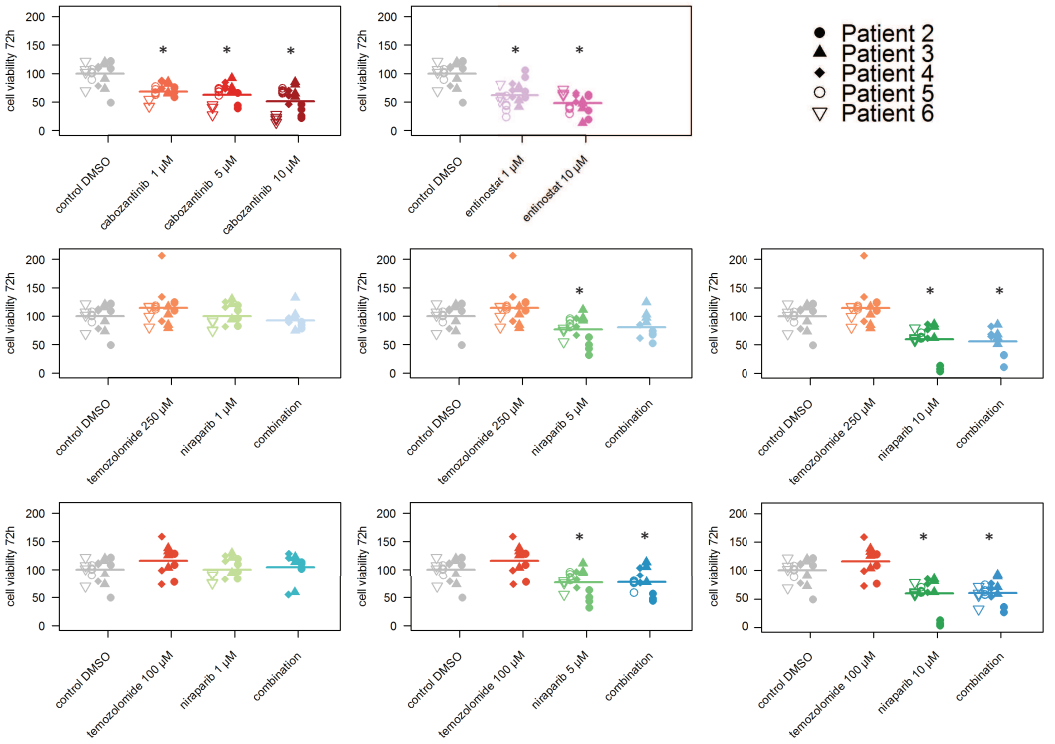

* Significant decrease of cell viability compared to control DMSO

Figure 12